Monthly Notices
of the
ROYAL ASTRONOMICAL SOCIETY

MNRAS **435,** 3654–3666 (2013)
Advance Access publication 2013 September 16

doi:10.1093/mnras/stt1557

Newly discovered globular clusters in NGC 147 and NGC 185 from PAndAS

J. Veljanoski,[1]⋆ A. M. N. Ferguson,[1] A. P. Huxor,[2] A. D. Mackey,[3] C. K. Fishlock,[3] M. J. Irwin,[4] N. Tanvir,[5] S. C. Chapman,[4] R. A. Ibata,[6] G. F. Lewis[7] and A. McConnachie[8]

[1]*Institute for Astronomy, University of Edinburgh, Royal Observatory, Blackford Hill, Edinburgh EH9 3HJ, UK*
[2]*Zentrum für Astronomie, Astronomisches Rechen-Institut Mönchhofstraße 12-14, D-69120 Heidelberg, Germany*
[3]*Research School of Astronomy & Astrophysics, Australian National University, Mt. Stromlo Observatory, Cotter Road, Weston Creek, ACT 2611, Australia*
[4]*Institute of Astronomy, Madingley Road, Cambridge CB3 0HA, UK*
[5]*Department of Physics & Astronomy, University of Leicester, Leicester LE1 7RH, UK*
[6]*Observatoire de Strasbourg, 11, rue de l'Université, F-67000 Strasbourg, France*
[7]*Institute of Astronomy, School of Physics, University of Sydney, NSW 2006, Australia*
[8]*NRC Herzberg Institute of Astrophysics, 5071 West Saanich Road, Victoria, British Columbia V9E 2E7, Canada*

Accepted 2013 August 16. Received 2013 August 15; in original form 2013 February 19

ABSTRACT

Using data from the Pan-Andromeda Archaeological Survey (PAndAS), we have discovered four new globular clusters (GCs) associated with the M31 dwarf elliptical (dE) satellites NGC 147 and NGC 185. Three of these are associated with NGC 147 and one with NGC 185. All lie beyond the main optical boundaries of the galaxies and are the most remote clusters yet known in these systems. Radial velocities derived from low-resolution spectra are used to argue that the GCs are bound to the dwarfs and are not part of the M31 halo population. Combining PAndAS with United Kingdom Infrared Telescope (UKIRT)/WFCAM (Wide-Field Camera) data, we present the first homogeneous optical and near-IR photometry for the entire GC systems of these dEs. Colour–colour plots and published colour–metallicity relations are employed to constrain GC ages and metallicities. It is demonstrated that the clusters are in general metal poor ([Fe/H] < -1.25 dex), while the ages are more difficult to constrain. The mean $(V - I)_0$ colours of the two GC systems are very similar to those of the GC systems of dEs in the Virgo and Fornax clusters, as well as the extended halo GC population in M31. The new clusters bring the GC-specific frequency (S_N) to ∼9 in NGC 147 and ∼5 in NGC 185, consistent with values found for dEs of similar luminosity residing in a range of environments.

Key words: galaxies: globular clusters: general – galaxies: individual: NGC 147 – galaxies: individual: NGC 185.

1 INTRODUCTION

Globular clusters (GCs) are ubiquitous in massive galaxies and their properties are believed to contain important clues about the galaxy assembly process. GCs are thought to form during major star-forming episodes which occur in the early Universe, as well as in subsequent major merger events (e.g. West et al. 2004; Brodie & Strader 2006). Their relative ages and metallicities therefore help constrain the star formation time-scale of the host galaxies in which they reside. GCs can also be accreted on to galaxies alongside their hosts in minor mergers. At present, we witness the Sagittarius dwarf spheroidal galaxy being accreted on to the Milky Way (MW) while donating at least five GCs to the MW GC system (e.g. Bellazzini, Ferraro & Ibata 2003; Law & Majewski 2010). Furthermore, almost 80 per cent of the outer halo GCs in M31 lie on top of stellar streams supporting an accretion origin for most of them (Mackey et al. 2010b). Studying the GC systems of satellite galaxies is not just interesting in its own right but can also give insight into how the GC systems of more massive galaxies are assembled.

Detailed study of GCs in satellite galaxies is uniquely accessible within the Local Group (LG) since individual stars can be easily resolved from both space and the ground (e.g. Mackey et al. 2006, 2010a; Dotter, Sarajedini & Anderson 2011). Identifying LG GCs does not need to rely on colour and magnitude criteria alone, as almost any GC candidate can be visually confirmed, effectively removing the possibility of contamination. Two particularly interesting LG satellites are the dwarf ellipticals (dEs) NGC 147 and

⋆E-mail: jv@roe.ac.uk

© 2013 The Authors
Published by Oxford University Press on behalf of the Royal Astronomical Society

Downloaded from http://mnras.oxfordjournals.org/ at The Australian National University on December 20, 2013

NGC 185. Amongst the brightest of the LG dwarf galaxies, they reside in the outer halo of M31 at projected galactocentric radii of ∼100 kpc, and 3D distances of 118^{+15}_{-15} kpc and 181^{+25}_{-20} kpc, respectively (Conn et al. 2012). For reference, taking the halo core radius of M31 to be ∼5 kpc (Gilbert et al. 2012), the 3D distances of NGC 147 and NGC 185 correspond to ∼24 and ∼36 core radii, respectively. It has been argued that the two systems may form a physical binary (van den Bergh 1998; Geha et al. 2010) although this claim has been questioned (Battinelli & Demers 2004; Watkins, Evans & van de Ven 2013). The stellar populations and star formation histories of these two dwarf galaxies have been extensively studied (e.g. Lee, Freedman & Madore 1993; Young & Lo 1997; Butler & Martínez-Delgado 2005; Davidge 2005; McConnachie et al. 2005). Despite their initial similarities, they exhibit some notable differences. NGC 147 is a typical dE composed primarily of old stars and is dust and gas free (Young & Lo 1997). However, NGC 185 has a substantial number of intermediate-age stars (Martínez-Delgado, Aparicio & Gallart 1999), as well as gas and dust (Young 2001). Bender, Paquet & Nieto (1991) found NGC 147 to be rotating, while NGC 185 to be entirely pressure supported. In contrast, Geha et al. (2010) found both galaxies to have significant internal rotation through the study of stars out to 8 effective radii.

Previous studies have discovered a number of GCs in NGC 147 and NGC 185, all of which lie in or near the main bodies of these systems (Baade 1944; Hodge 1976; Ford, Jacoby & Jenner 1977; Sharina & Davoust 2009). Thorough photometric (Baade 1944; Hodge 1974) and spectroscopic studies (Da Costa & Mould 1988; Sharina, Afanasiev & Puzia 2006; Sharina & Davoust 2009) have been undertaken on these clusters, some of which are the brightest GCs known to reside in LG dwarf galaxies. This work has shown that in general the GCs hosted by NGC 147 and NGC 185 are old (>7 Gyr) and metal poor ([Fe/H] < −0.8 dex). However, it is becoming increasingly appreciated that GCs can reside far from their host galaxies (e.g. Galleti et al. 2004; Hwang et al. 2011; Huxor et al. 2011, 2012; Jang et al. 2012) and this has motivated us to explore the remote environs of these systems to search for additional members. In this paper, we present the discovery of four outlying GCs, three of which belong to NGC 147 while one is hosted by NGC 185. We derive the first homogeneous optical and near-IR photometry for the entire GC populations of the dEs which we use to constrain their ages and metallicities. In addition, we present radial velocity measurements for the newly discovered GCs which are used to argue that they are bound to the dEs themselves as opposed to the extended M31 halo system.

For the purposes of this work, we adopt distance moduli of 24.26 ± 0.06 and $23.96^{+0.07}_{-0.06}$ for NGC 147 and NGC 185, respectively (Conn et al. 2012). The absolute magnitudes of these dwarf galaxies are taken from McConnachie (2012) and are −14.6 ± 0.1 and −14.8 ± 0.1 for NGC 147 and NGC 185, respectively.

The paper has the following structure. The observations and data reduction are described in Section 2. Sections 3 and 4 present the discovery and the photometric data of all known GCs in these two dwarf galaxies. The radial velocities of the newly discovered GCs are presented in Section 5. In Section 6, the optical and near-IR colours are used to constrain ages and metallicities and we compare some properties of the GCs to those observed in other systems. The content of the paper is summarized in Section 7. Finally, in Appendix A we present a review of the discovery history of the GCs found around NGC 147 and NGC 185, pointing out certain inconsistencies in the literature, with the aim being to reduce the possibility of confusion when studying these systems in the future.

2 OBSERVATIONS AND DATA REDUCTION

2.1 Optical data

The optical imaging used in this work was taken as part of the recently completed 'Pan-Andromeda Archaeological Survey' (PAndAS; McConnachie, Irwin & Ibata 2009). This optical imaging survey mapped M31 and its close companion M33 with the wide-field MegaCam camera (Boulade et al. 2003) on the Canada–France–Hawaii Telescope (CFHT). In brief, the detector consists of a mosaic of 36 CCDs, giving a total field of view of ≈1deg^2, and with a pixel scale of 0.187 arcsec. The survey consisted of ≈400 distinct pointings, covering an area of ∼380 deg^2 and extending to a projected radius of ∼150 kpc from the centre of M31. PAndAS was undertaken in the *g* and *i* bands. The observations were taken in good photometric conditions, with typical seeing <0.8 arcsec, and reaching a depth of $g \sim 25.5$ and $i \sim 24.5$ with signal-to-noise ratio (S/N) of 10.

The MegaCam data were initially reduced by CFHT staff using the *'Elixir'* pipeline which performs the standard bias, flat-field and fringe corrections, and determines the photometric zero-point. The typical night-to-night variation of the zero-point is around 1–2 per cent (Regnault et al. 2009). The data are further processed by the Cambridge Astronomy Survey Unit,[1] as described in full detail by McConnachie et al. (2010).

2.2 Near-IR data

The near-IR data were taken in 2008 October, as part of a survey designed to look at red stellar populations in LG galaxies. It used the Wide-Field Camera (WFCAM; Casali et al. (2007)) on the United Kingdom Infrared Telescope (UKIRT). This instrument has a pixel scale of 0.4 arcsec, and the detectors are arranged such that four dithered pointings are aligned to cover a square of 0.75 deg^2. The observations were done in three near-IR bands, *J*, *H* and *K*, with seeing of 0.8 arcsec or better, using the microstepping option to improve the pixel sampling to 0.2 arcsec.

The data were reduced with a pipeline designed by the Cambridge Astronomy Survey Unit, performing the usual dark-correction, flat-fielding, crosstalk removal, systematic noise and sky removal. The pipeline, which is part of the VDFS,[2] also does full astrometric and photometric calibration based on the 2MASS point source catalogue and is described in Cioni et al. (2008) and Hodgkin et al. (2009). The nightly zero-point variation on photometric nights is <1 per cent. The reduced images were stacked and microstepped to produce individual detector frames. These were then resampled to form a 0.333 arcsec per pixel science mosaic (Irwin et al. 2004).

2.3 Spectroscopic data

Low-resolution spectra of the new GCs were obtained during two nights in 2010 September using the Intermediate dispersion Spectrograph and Imaging System (ISIS) instrument mounted on the *William Herschel Telescope* (*WHT*). Several exposures were made of each object with varying integration time depending on the brightness of the target. The specifics of these observations are shown in Table 1.

The ISIS instrument employs two detectors, each attached to a separate 'arm' of the spectrograph. The blue arm used the R600B grating and was selected to cover the wavelength range between

[1] http://casu.ast.cam.ac.uk
[2] VISTA data flow system.

Downloaded from http://mnras.oxfordjournals.org/ at The Australian National University on December 20, 2013

Table 1. Journal of the spectroscopic observations.

ID	Date of obs.	Number of exposures	Integration time per exposure (s)
PA-N147-1	10/09/2010	4	800
PA-N147-2	10/09/2010	3	800
PA-N147-3	10/09/2010	3	1500
PA-N185	11/09/2010	4	1800

3500 and 5100 Å with a dispersion of 0.45 Å pixel^{-1}. The red arm used the R600R grating and was selected to cover the wavelength range between 7400 and 9100 Å with a dispersion of 0.79 Å pixel^{-1}. The slit width was 2 arcsec throughout the observations and no binning was applied in either the spectral or spatial directions. The S/N per pixel of the spectra observed with the blue arm varies between 7 and 22, while for the red arm between 11 and 30. The observations were undertaken under generally good atmospheric conditions with the seeing varying from 0.7 to 1.6 arcsec over the two nights.

The reduction of the spectra (bias subtraction, flat-fielding, illumination correction) was done with standard tasks that are part of the CCDRED package within IRAF.[3] Following initial processing, the spectra were traced and extracted with a 4 arcsec aperture using the APALL task in IRAF. For each exposure, a background region was interactively selected and the sky was fit and subtracted with a second-order Chebyshev polynomial. The sky-subtraction generally worked well, with only the strongest lines in the red spectra leaving some residuals. The spectra were traced using a third order cubic-spline function and extracted with the optimal variance weighting option of APALL.

Wavelength calibration of the 1D spectra was based on He–Ne–Ar lamp exposures obtained before and after each target exposure. The arc spectra were extracted using the same APALL settings as the target objects that they are used to calibrate. Typically ∼90 blue and ∼25 red lines were identified and the dispersion solution was fit with a third -order cubic-spline function. The rms residuals of these fits were 0.05 ± 0.01 Å in the blue and 0.02 ± 0.01 Å in the red. The IRAF DISPCOR task was then used to assign the wavelength solutions to the target GC spectra. The positions of sky lines were used to verify that the wavelength calibration was accurate to 0.08 Å with no systematic shifts. The wavelength-calibrated 1D spectra for each object were stacked using inverse variance weights to produce final science spectra. Finally, the continuum-normalized spectra are shown in Fig. 1.

3 DISCOVERY

At the distance of NGC 147 and NGC 185, GCs are partially resolved into stars at optical wavelengths and can be easily identified. Visual inspection of the area surrounding the two dEs was conducted by three of us (AH, DM, JV) and resulted in the discovery of four new GCs, three belonging to NGC 147, and one to NGC 185. We refer to these objects with the prefix 'PA'. Images of these objects in the g and K bands are shown in Fig. 2. For completeness and comparison, the previously known GCs are also included. Table 2 lists the coordinates, projected galactocentric radii ($R_{\rm proj}$) and Galactic reddening coefficients, $E(B-V)$, from Schlegel, Finkbeiner & Davis (1998) for all clusters. While this paper was in preparation, we found various inconsistencies in the literature regarding the nomenclature of the previously known GCs in NGC 147 and NGC 185. These have been described in Appendix and we have made an effort to rectify these inconsistencies throughout the paper whenever possible.

Our search is based on homogeneous and sensitive imagery covering a very large fraction of the areas around these two dEs. However, there are two sources of incompleteness that need to be considered. One is due to spatial incompleteness, arising from the many gaps between the imaging CCDs in the MegaCam focal plane, and the gaps coming from the imperfect tiling of the observations. GCs are sufficiently small on the sky that they could be missed were they to land in such a gap. The other source of incompleteness is due to our ability to visually detect GCs. We assessed incompleteness using the methodology we devised for our M31 halo GC search, which will be discussed in full detail in Huxor et al. (in preparation). Here we provide only a brief overview.

To quantify the spatial incompleteness, we calculate the area lost due to gaps in the imagery. First, we used the WCS information in the image headers to determine the RA and Dec. boundaries of each of the 36 CCDs in a given MegaCam pointing. We then generated a set of random points around the two galaxies with a density of ∼100 arcmin^{-2}. The 'observed' area was simply calculated by dividing the number of points which fell within the RA and Dec. boundaries by the total number generated. This test indicates that the fractions of NGC 147 and NGC 185 that are imaged out to a circular radius of 15 kpc are 96.3 per cent and 93.5 per cent, respectively.

To quantify our ability to detect GCs through visual inspection, we generated a suite of artificial GCs using the SIMCLUST (Deveikis et al. 2008) and SKYMAKER (Bertin 2009) software packages. The clusters were generated with a range of luminosity and concentration[4] and were embedded within field star backgrounds of varying density. Thumbnails of these generated clusters were then visually inspected by one of us (AH) who decided if a cluster was present or not based on the same criteria we applied to the real data. Using this method, we found that, for most values of concentration, the GC recovery is 100(50) per cent complete down to $M_V \approx -5.3(-4.1)$ around NGC 147. Around NGC 185, the search is 100(50) per cent complete down to $M_V \approx -5.0(-3.8)$. For reference, these limits indicate that we would be able to detect most, if not all, of the MW Palomar type clusters. Indeed, of the 13 such objects known in the MW that have available absolute integrated V magnitudes, 10 of them are brighter than -5.0, while 11 are brighter than -4.0 (Harris 1996). We would not be able to detect the Koposov clusters which have $M_V \sim -1$ (Koposov et al. 2007), although these are difficult to find even in the MW. It thus seems likely that we have uncovered all the luminous remote GCs around these two systems.

Fig. 3 shows the spatial distribution of GCs in the two galaxies where it can readily be seen that the newly discovered GCs are much more remote than the known populations. Given this, it is possible that some of them might be bound to M31 rather than to NGC 147 or NGC 185. This could be especially true for PA-N147-3 which is located at projected radius of 6.6 kpc from the centre of its host galaxy NGC 147.

[3] IRAF is distributed by the National Optical Astronomy Observatories, which are operated by the Association of Universities for Research in Astronomy, Inc., under cooperative agreement with the National Science Foundation.

[4] The concentration is defined as $c = \log(r_{\rm t}/r_{\rm c})$, where $r_{\rm t}$ and $r_{\rm c}$ are the cluster tidal and core radii, respectively, assuming a King (1962) profile for its radial surface density.

Downloaded from http://mnras.oxfordjournals.org/ at The Australian National University on December 20, 2013

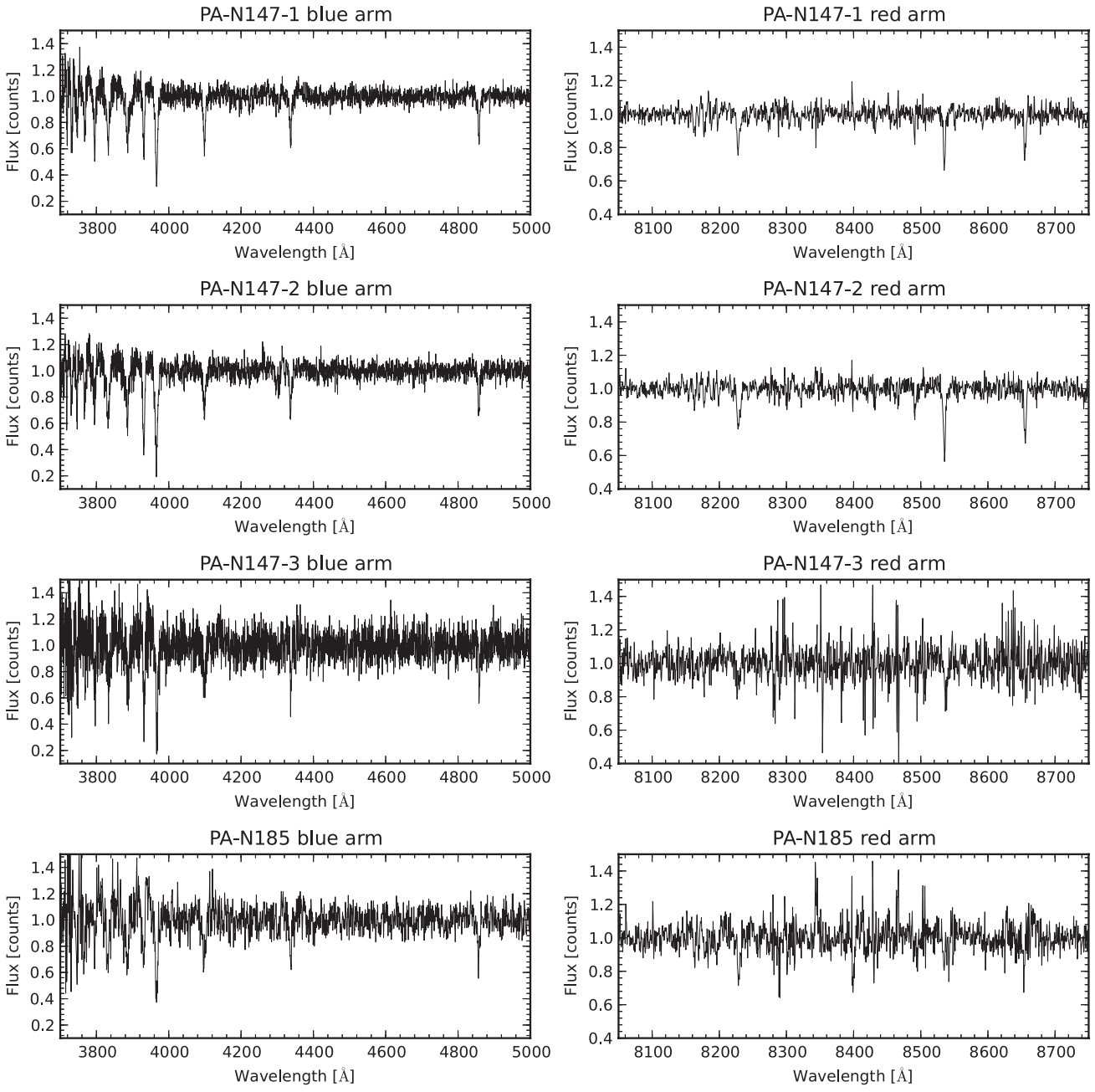

Figure 1. Wavelength calibrated, normalized spectra of the newly discovered GCs. The left (right) panels show the spectra obtained with the blue (red) arm of the ISIS instrument.

To examine this possibility, we calculate the probability of finding a genuine M31 GC projecting as close to NGC 147 and NGC 185 as the new objects we have found. We consider a circular annulus spanning 90–110 kpc in projected radius from M31's centre, the size of which is chosen to comfortably encompass the positions and extents of NGC 147 and NGC 185. Inside the annulus there are eight M31 GCs excluding the new objects around NGC 147 and NGC 185 (Mackey et al., in preparation), which in turn equals a number density of 6.4×10^{-4} clusters kpc^{-2}. We define a search radius of 7 kpc and 2 kpc around NGC 147 and NGC 185, respectively, chosen to be slightly larger than the GCs that have the largest projected distance from the centres of these systems. On average one would expect to find 0.008 GCs within a circular area of 2 kpc radius and 0.098 GCs within a 7 kpc circular radius. The Poisson probability of finding one or more M31 GCs within a 2 kpc radius of NGC 185 and within a 7 kpc radius of NGC 147 is 1 per cent and 10 per cent, respectively. The probability of finding three or more GCs within a 7 kpc radius of NGC 147 drops to 0.01 per cent. The conclusion from this analysis is that, in the absence of other information, there is a small chance that at least one of the newly discovered GCs around NGC 147 could be part of the M31 halo GC system, while the newly discovered cluster around NGC 185 almost certainly belongs to its apparent host galaxy. It is also worth noting that two of the newly discovered GCs around NGC 147 appear to lie on top of tidal tails which emanate from this system (Lewis et al. 2013, Irwin et al., in preparation).

Downloaded from http://mnras.oxfordjournals.org/ at The Australian National University on December 20, 2013

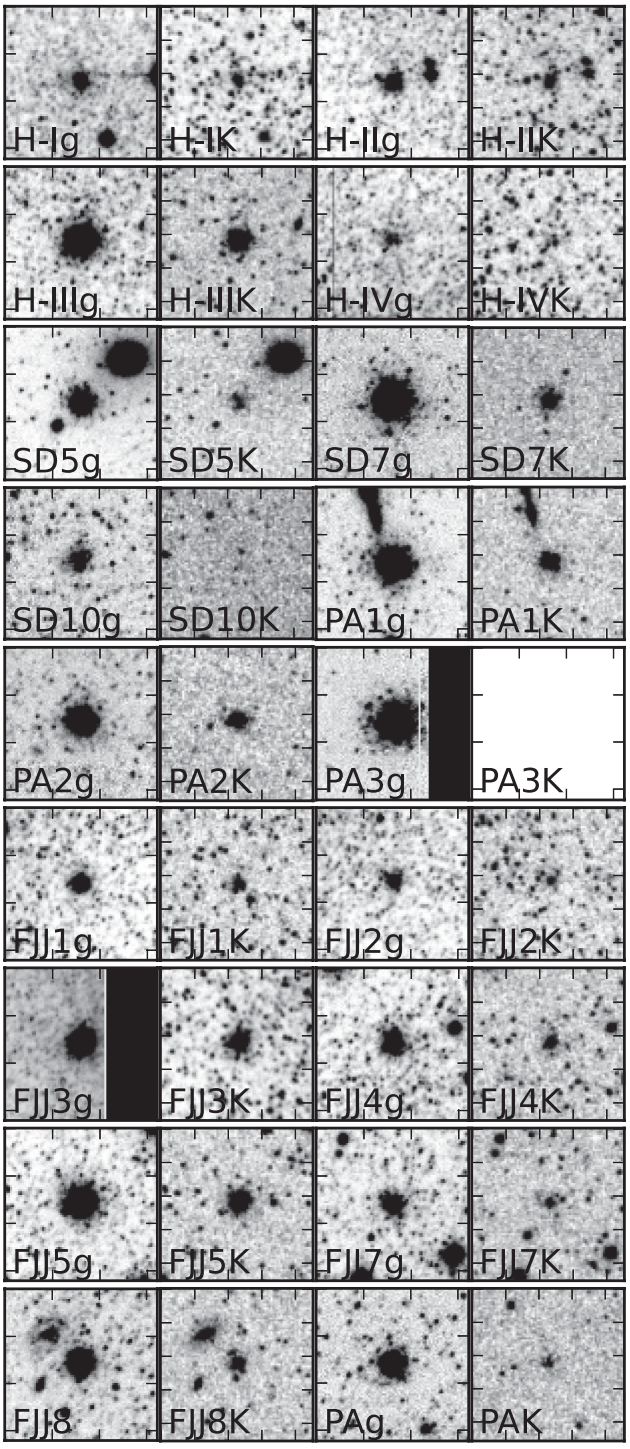

Figure 2. *g*- and *K*-band images of all the clusters in NGC 147 and NGC 185. Each image is 30 × 30 arcsec wide. North is up and east is left. Cluster PA-N147-3 falls outside the IR survey hence no *K*-band image is shown. Note that the scale in each cutout has been manually set to make each cluster easily visible.

4 PHOTOMETRY

Integrated photometry of all the GCs in these two dwarf galaxies was done with the PHOT task within IRAF. The centroid algorithm within the PHOT task was used to determine accurate centres of the clusters by computing the intensity weighted means of the marginal profiles along the physical *x*- and *y*-axes in the *g*-band images. Circular apertures were then used to sum the total flux. Concentric 'sky' annuli around the photometric apertures, with typical width of ∼7 arcsec, were employed to determine the mean background flux contribution. The exact sizes of the background annuli were carefully selected to avoid pollutants such as bright foreground stars and background galaxies. As some of these clusters lie in very crowded fields, detailed tests were performed to ensure that the background contribution was reliably subtracted.

Table 2. Coordinates, projected radii and Galactic reddening coefficients of GCs in NGC 147 and NGC 185.

ID	RA(J2000) (h m s)	Dec. (J2000) (d m s)	R_{proj} (kpc)	$E(B-V)$ (mag)
Hodge I	00 33 12.2	+48 30 32.3	0.03	0.17
Hodge II	00 33 13.6	+48 28 48.7	0.34	0.17
Hodge III	00 33 15.2	+48 27 23.1	0.64	0.17
Hodge IV	00 33 15.0	+48 32 09.6	0.38	0.17
SD-GC5	00 32 22.9	+48 25 49.0	1.93	0.18
SD-GC7	00 32 22.2	+48 31 27.0	1.72	0.17
SD-GC10	00 32 47.2	+48 32 10.7	0.92	0.17
PA-N147-1	00 32 35.3	+48 19 48.0	2.53	0.15
PA-N147-2	00 33 43.3	+48 38 45.0	2.04	0.16
PA-N147-3	00 34 10.0	+49 02 39.0	6.97	0.16
FJJ I	00 38 42.7	+48 18 40.4	0.53	0.17
FJJ II	00 38 48.1	+48 18 15.9	0.45	0.17
FJJ III	00 39 03.8	+48 19 57.5	0.20	0.19
FJJ IV	00 39 12.2	+48 22 48.2	0.64	0.19
FJJ V	00 39 13.4	+48 23 04.9	0.70	0.19
FJJ VII	00 39 18.4	+48 23 03.6	0.81	0.19
FJJ VIII	00 39 23.7	+48 18 45.1	0.83	0.17
PA-N185	00 38 18.8	+48 22 04.0	1.20	0.18

For each GC we constructed a curve-of-growth by measuring the flux in concentric apertures of increasing radius. The final photometric aperture size was set to be the point at which the cumulative flux becomes flat. This did not work for clusters in the very dense fields, where we adopted an aperture size based mainly on visual inspection, even though the curve-of-growth was not flat. To reduce background contamination, a smaller aperture of 3.5 arcsec was used when measuring colours, valid if we assume that no colour gradients are present within the GCs. Aperture sizes for both colours and magnitudes were matched to be the same in the optical and near-IR data. For all photometric measurements, the instrumental magnitudes were zero-point calibrated, corrected for atmospheric extinction and corrected for Galactic reddening using the Schlegel et al. (1998) maps interpolated to the position of each GC. Tables 3 and 4 list the extinction-corrected magnitudes and colours of all GCs in NGC 147 and NGC 185.

Some objects required special treatment. In the cases of Hodge II and SD-GC5, a mask was applied consistently to all filters in order to exclude bright contaminating objects that entered the photometric aperture. The cluster PA-N147-3 was split between two separate CCD frames in the optical data. To account for this, we summed the flux within rectangular apertures on each frame and combined them; this strictly represents a lower limit on the total magnitude of this object. This same cluster has the largest projected radius of all GCs in our sample and it falls outside the near-IR survey area, meaning no near-IR measurement is possible. The cluster SD-10 was not detected in the near-IR imaging and the corresponding near-IR magnitudes listed provide upper limits on its brightness. The GC FJJ III lies very close to the edge of the chip in the *g* band,

Downloaded from http://mnras.oxfordjournals.org/ at The Australian National University on December 20, 2013

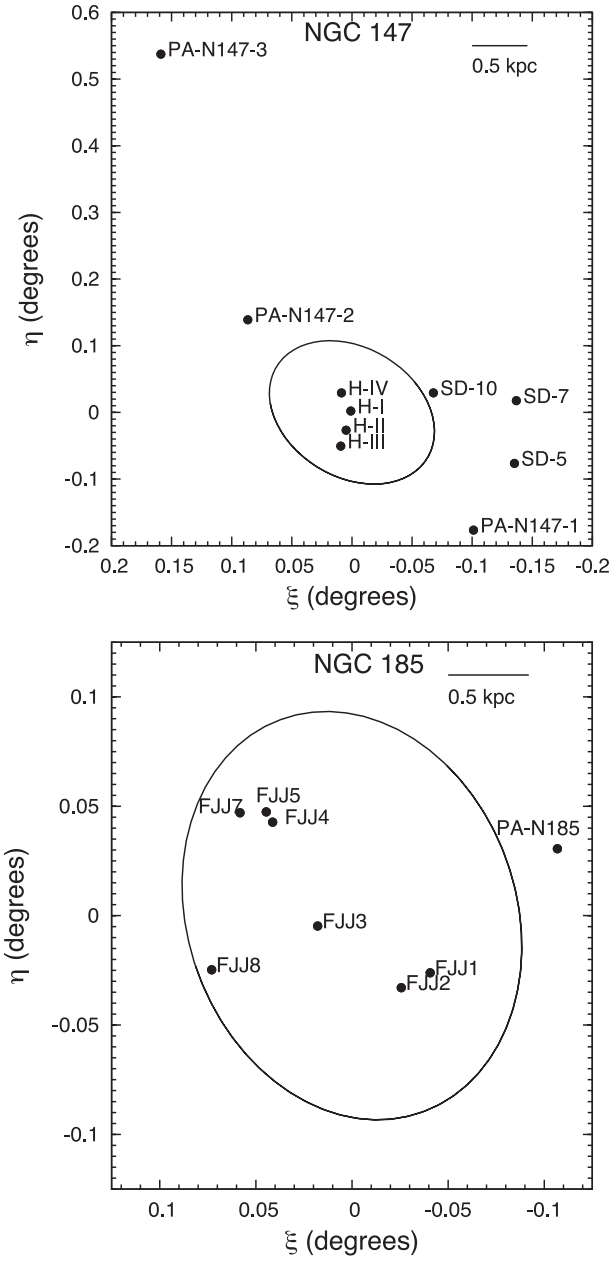

Figure 3. Schematic view of NGC 147 (top panel) and NGC 185 (bottom panel) along with their GCs in standard coordinates. The centres of NGC 147 and NGC 185 are taken to be RA = 00:33:12.1, Dec. = 48:30:32 and RA = 00:38:58.0, Dec. = 48:20:15, respectively (McConnachie 2012). The ellipses represent the 25th magnitude *B*-band isophote taken from Corwin, Buta & de Vaucouleurs (1994). The new GCs lie further away from the centre of their host galaxies than the known populations. On the top panel 'H' stands for 'Hodge' and 'SD' stands for 'GC-SD'.

while it is split between two chips in the *i* band. For the optical photometry of this cluster, previously published data obtained with the Isaac Newton Telescope Wide Field Camera (INT/WFC) were used (McConnachie et al. 2005). This was not possible for PA-N147-3 as it falls outside the area covered by the INT survey. The INT/WFC survey uses the Johnson V and Gunn *i* passbands, which are on the Vega scale. Hence the magnitudes of FJJ III were converted to the CFHT/MegaCam system, which is on the AB scale, via transformations presented in Ibata et al. (2007).

To allow comparison with other work, Tables 3 and 4 also contain magnitudes and colours converted to the more widely used Johnson/Cousins filters. The CFHT/MegaCam data were transformed into the standard V and I system via corrected relations from Huxor et al. (2008):[5]

$$g_1 = g + 0.092$$

$$i_1 = i - 0.401$$

$$\mathrm{V} = g_1 - 0.42(g_1 - i_1) + 0.04(g_1 - i_1)^2 + 0.10$$

$$\mathrm{I} = i_1 - 0.08(g_1 - i_1) + 0.06.$$

These relations were derived for the i' filter used with CFHT/MegaCam pre-2007 June, while in 2007 October a new *i* filter was installed on this instrument. The data used in this paper were taken with the new *i* filter and so before transforming the MegaCam data to the standard V and I filters, conversion from the new *i* to the old i' filter was done using the relation derived in Ibata et al. (in preparation).

In deriving magnitudes and colours, various uncertainties are included and appropriately combined. The instrumental magnitude uncertainties reported by IRAF are small, as the clusters are much brighter than the background sky. For GCs lying within the main optical bodies of their host dwarf galaxies, the main source of uncertainty comes from the local background, which is contaminated by resolved stars from the host galaxy as well as the underlying diffuse light. To assess the uncertainty in the background, we randomly placed 10 apertures around each cluster sampling the local sky. While the apertures include the resolved field star component and the diffuse light of the host dwarf galaxies, we excluded obvious contaminants such as background galaxies or foreground MW stars. The sky apertures were chosen to have the same size as the magnitude and colour apertures that we used to photometer the GCs. We found the standard deviation of all 10 sky measurements around each cluster, and added this in quadrature to the instrumental and zero-point errors. Furthermore, every conversion between filters introduces an additional uncertainty to the derived magnitudes and colours that we account for as well.

5 RADIAL VELOCITIES

Heliocentric radial velocities of the newly discovered GCs were measured using a chi-squared minimization technique between the GC spectra and spectra of high S/N radial velocity template stars and clusters (Veljanoski et al. 2013). This method is analogous to the standard cross-correlation technique, and produces similar results. The advantage of doing a chi-square minimization is that this technique uses the uncertainties in both the template and target spectra, which helps to eliminate spurious features, and differentiate between genuine spectral lines and poorly subtracted sky lines, which might be important in the case of faint targets.

Because both ISIS arms were used during the observations, two independent velocity measurements could be made for each GC. The values reported in Table 5 represent the error-weighted averages of the individual measurements from the blue and red spectra. For comparison, the heliocentric radial velocities of NGC 147 and NGC 185 themselves are also shown (Geha et al. 2010).

[5] Note that the transformation equations in that paper were incorrectly written, but the magnitudes derived were based on the correct equations.

Downloaded from http://mnras.oxfordjournals.org/ at The Australian National University on December 20, 2013

Table 3. Photometry for the NGC 147 and NGC 185 GCs. $M_{V,0}$ was calculated assuming the line-of-sight distance to the clusters is the same as to their host galaxies. Superscripts refer to (1) the presence of masked bright objects in the photometric aperture, (2) the magnitude is a lower limit as the cluster is split between CCD frames and was measured in a rectangular aperture, (3) the photometry is measured from INT imaging.

ID	Aperture (arcsec)	g_0 (mag)	i_0 (mag)	J_0 (mag)	H_0 (mag)	K_0 (mag)	V_0 (mag)	I_0 (mag)	$M_{V,0}$ (mag)
Hodge I	6.5	17.17 ± 0.04	16.31 ± 0.02	14.84 ± 0.02	14.25 ± 0.02	14.13 ± 0.03	16.86 ± 0.03	15.92 ± 0.02	-7.40
Hodge II[1]	4.6	17.79 ± 0.04	17.07 ± 0.04	15.93 ± 0.02	15.30 ± 0.02	15.14 ± 0.02	17.53 ± 0.03	16.71 ± 0.04	-6.73
Hodge III	7.4	16.29 ± 0.03	15.65 ± 0.02	14.71 ± 0.01	14.15 ± 0.01	14.18 ± 0.01	16.05 ± 0.02	15.29 ± 0.02	-8.21
Hodge IV	4.6	18.83 ± 0.04	17.81 ± 0.03	16.55 ± 0.03	15.98 ± 0.03	15.94 ± 0.04	18.48 ± 0.03	17.41 ± 0.03	-5.78
GC-SD5[1]	5.6	17.83 ± 0.02	17.20 ± 0.01	16.36 ± 0.02	15.81 ± 0.02	15.77 ± 0.03	17.60 ± 0.01	16.85 ± 0.01	-6.66
GC-SD7	7.4	16.73 ± 0.01	16.03 ± 0.01	15.03 ± 0.01	14.49 ± 0.01	14.43 ± 0.02	16.47 ± 0.01	15.66 ± 0.01	-7.79
GC-SD10	4.6	19.59 ± 0.01	18.86 ± 0.01	$>17.84 \pm 0.06$	$>17.30 \pm 0.06$	$>17.22 \pm 0.12$	19.32 ± 0.01	18.49 ± 0.02	-4.94
PA-N147-1	6.5	16.72 ± 0.01	16.09 ± 0.01	15.15 ± 0.01	14.69 ± 0.01	14.64 ± 0.02	16.49 ± 0.01	15.74 ± 0.01	-7.77
PA-N147-2	6.5	17.11 ± 0.01	16.44 ± 0.01	15.37 ± 0.01	14.89 ± 0.01	14.86 ± 0.02	16.87 ± 0.01	16.08 ± 0.01	-7.39
PA-N147-3		17.17 ± 0.01[2]	17.63 ± 0.01[2]	...	...	...	17.38 ± 0.01[2]	17.42 ± 0.01[2]	-6.88[2]
FJJ I	4.6	17.96 ± 0.03	17.22 ± 0.02	15.24 ± 0.02	15.39 ± 0.03	15.06 ± 0.02	17.70 ± 0.03	16.85 ± 0.03	-6.26
FJJ II	4.6	18.28 ± 0.04	17.49 ± 0.03	15.59 ± 0.03	15.75 ± 0.03	15.73 ± 0.04	18.00 ± 0.03	17.12 ± 0.03	-5.96
FJJ III	7.4	16.20 ± 0.29[3]	15.55 ± 0.11[3]	13.80 ± 0.02	14.02 ± 0.02	13.94 ± 0.01	15.99 ± 0.17[3]	15.14 ± 0.11[3]	-7.97[3]
FJJ IV	5.6	17.58 ± 0.03	17.00 ± 0.02	15.24 ± 0.02	15.53 ± 0.03	15.60 ± 0.04	17.37 ± 0.02	16.65 ± 0.02	-6.59
FJJ V	7.4	16.38 ± 0.03	15.66 ± 0.02	13.85 ± 0.01	14.09 ± 0.02	14.00 ± 0.01	16.12 ± 0.02	15.30 ± 0.02	-7.84
FJJ VII	4.6	18.36 ± 0.02	17.62 ± 0.01	15.80 ± 0.02	16.06 ± 0.03	16.07 ± 0.04	18.10 ± 0.02	17.25 ± 0.02	-5.85
FJJ VIII	4.6	17.29 ± 0.01	16.59 ± 0.01	14.82 ± 0.01	15.08 ± 0.02	15.09 ± 0.02	17.04 ± 0.01	16.23 ± 0.01	-6.92
PA-N185	4.6	18.65 ± 0.01	17.98 ± 0.01	16.23 ± 0.03	16.54 ± 0.04	16.39 ± 0.06	18.41 ± 0.01	17.62 ± 0.01	-5.55

Table 4. Colours for the NGC 147 and NGC 185 GCs. All measurements are done within a 3.5 arcsec aperture radius in order to minimize background contamination. Colours of PA-N147-3 cannot be calculated as different portions of the cluster have been measured on the optical imaging and it was not imaged in the near-IR. Superscripts refer to (1) the presence of masked bright objects in the photometric aperture, (2) the photometry is measured from INT imaging.

ID	$(g-i)_0$ (mag)	$(g-J)_0$ (mag)	$(g-H)_0$ (mag)	$(g-K)_0$ (mag)	$(V-I)_0$ (mag)	$(V-K)_0$ (mag)
Hodge I	0.72 ± 0.04	1.97 ± 0.04	2.51 ± 0.04	2.59 ± 0.04	0.83 ± 0.04	2.33 ± 0.03
Hodge II[1]	0.68 ± 0.07	1.75 ± 0.05	2.30 ± 0.05	2.35 ± 0.05	0.79 ± 0.07	2.11 ± 0.04
Hodge III	0.61 ± 0.04	1.57 ± 0.04	2.07 ± 0.04	2.10 ± 0.04	0.73 ± 0.04	1.87 ± 0.03
Hodge IV	0.96 ± 0.05	2.31 ± 0.05	2.89 ± 0.05	2.96 ± 0.05	1.02 ± 0.04	2.62 ± 0.05
GC-SD5	0.60 ± 0.02	1.46 ± 0.03	2.00 ± 0.02	2.03 ± 0.03	0.73 ± 0.01	1.81 ± 0.03
GC-SD7	0.67 ± 0.01	1.69 ± 0.02	2.22 ± 0.01	2.28 ± 0.02	0.78 ± 0.01	2.04 ± 0.02
GC-SD10	0.76 ± 0.02	$<1.83 \pm 0.06$	$<2.40 \pm 0.05$	$<2.25 \pm 0.11$	0.85 ± 0.02	$<1.98 \pm 0.11$
PA-N147-1	0.52 ± 0.01	1.60 ± 0.02	2.04 ± 0.01	2.14 ± 0.02	0.75 ± 0.01	1.91 ± 0.02
PA-N147-2	0.66 ± 0.01	1.70 ± 0.02	2.16 ± 0.02	2.20 ± 0.02	0.79 ± 0.01	1.97 ± 0.02
PA-N147-3	...	...	...	...	...	...
FJJ I	0.73 ± 0.04	2.64 ± 0.04	2.41 ± 0.04	2.55 ± 0.04	0.84 ± 0.04	2.30 ± 0.04
FJJ II	0.75 ± 0.05	2.63 ± 0.05	2.46 ± 0.05	2.52 ± 0.05	0.85 ± 0.04	2.25 ± 0.04
FJJ III[2]	0.67 ± 0.31	2.56 ± 0.29	2.30 ± 0.29	2.42 ± 0.29	0.86 ± 0.19	2.22 ± 0.16
FJJ IV	0.63 ± 0.04	2.39 ± 0.03	2.09 ± 0.04	2.10 ± 0.04	0.75 ± 0.04	1.87 ± 0.04
FJJ V	0.70 ± 0.03	2.52 ± 0.03	2.24 ± 0.03	2.31 ± 0.03	0.81 ± 0.03	2.06 ± 0.02
FJJ VII	0.73 ± 0.03	2.60 ± 0.03	2.34 ± 0.03	2.36 ± 0.04	0.84 ± 0.03	2.10 ± 0.03
FJJ VIII	0.69 ± 0.02	2.48 ± 0.02	2.22 ± 0.03	2.24 ± 0.02	0.80 ± 0.02	2.00 ± 0.02
PA-N185	0.68 ± 0.01	2.50 ± 0.03	2.22 ± 0.03	2.38 ± 0.04	0.80 ± 0.01	2.13 ± 0.04

The measured velocities of the new GCs can be used as another indicator of whether they are bound to the dEs or to M31. The velocity dispersion of M31 halo GCs that lie beyond 70 kpc in projection is $\sim$50 km s^{-1} (Veljanoski et al. 2013). Given the large difference between the radial velocities of the new NGC 147 GCs and that of M31 (-301 ± 4 km s^{-1}; Courteau & van den Bergh 1999), it is likely that they are hosted by the dwarf galaxy. This is not the case for PA-N185, as the difference between it and the M31 velocity is comparable to the M31 outer halo GC velocity dispersion. However, when combined with the probability arguments presented earlier, the velocity measurements strengthen the conclusion that the new GCs are probably members of the dE systems and not the M31 halo.

It is interesting to point out that the cluster PA-N147-3 projects in position halfway between NGC 147 and the newly discovered dwarf spheroidal Cass II (Conn et al. 2012; Irwin et al., in preparation). Furthermore, it has a similar radial velocity to Cass II, which is measured to be -139 ± 6 km s^{-1} (Collins et al. 2013). It is therefore possible that this GC could be a satellite of Cass II instead of NGC 147, or else not bound to either system. We postpone a detailed kinematical analysis of GCs within the NGC 147/185 subgroup until a later publication.

Downloaded from http://mnras.oxfordjournals.org/ at The Australian National University on December 20, 2013

Table 5. Heliocentric radial velocities and their uncertainties for the newly discovered GCs around NGC 147 and NGC 185. For comparison, the heliocentric velocities of NGC 147 and NGC 185 (Geha et al. 2010) are also shown.

ID	Radial velocity (km s^{-1})	Uncertainty (km s^{-1})
NGC 147	−193.1	0.8
PA-N147-1	−215	10
PA-N147-2	−219	10
PA-N147-3	−133	24
NGC 185	−203.8	1.1
PA-N185	−254	15

6 ANALYSIS

6.1 Ages and metallicities

We derive age and metallicity estimates for the two cluster samples using our integrated optical and NIR photometry. In principle, one can determine accurate ages and metallicities of GCs with high-quality spectroscopic data. However, our spectra have low S/N, and only two out of the four new GCs have spectra that are suitable for metallicity determination. Furthermore, as our goal is to present a homogeneous analysis of the sample, including objects for which we do not have spectra, we prefer to base our analysis on integrated photometry alone. Optical colours are well-known to suffer from an age–metallicity degeneracy; however the addition of near-IR measurements can greatly improve the situation (e.g. Puzia et al. 2002; Hempel et al. 2005; Chies-Santos et al. 2011). This is because of the different sensitivities to age and metallicity of the optical–optical and optical–near-IR colours. The optical g-band is most sensitive to stars near the main-sequence turn-off, the magnitudes of which are mostly driven by age. Conversely, the near-IR K band is most sensitive to red giant branch stars (Saviane et al. 2000; Yi et al. 2001). The $g - i$ and $g - K$ colours have similar sensitivity to age, but $g - K$ measures the temperature of the red giant branch which more reflects metallicity than age. Plotting these colours on a colour–colour diagram and comparing to simple stellar population (SSP) model tracks allow us to derive estimates of the age and metal content of each GC.

Various SSP models have been constructed to date (e.g. Maraston 1998; Bruzual & Charlot 2003; Marigo et al. 2008; Vazdekis et al. 2010). Despite improvements over time, discrepancies still exist between models. One of the largest intrinsic uncertainties in SSP models comes from the limited understanding of certain phases of advanced stellar evolution such as the thermally pulsating asymptotic giant branch (TP-AGB) phase. Different attempts to implement this phase have led to large differences in the near-IR fluxes. Stars in this phase are short-lived making calibration difficult (Girardi et al. 2010). Models having prominent TP-AGB phases cause the near-IR luminosity of objects to be overpredicted, but this only affects objects of young to intermediate ages (Kriek et al. 2010). Another problem related to each SSP model is the convergence of the isochrones in the metal-poor regime which produces large uncertainties in the derived properties.

Fig. 4 shows colour–colour diagrams constructed using the optical and near-IR photometry presented in Table 4. While the SSP model track shown here is from Marigo et al. (2008), we have checked that none of the results presented in this paper depends on the chosen SSP model. We resorted to using the native CFHT/Megacam rather than the more common Johnson/Cousins system in order to avoid uncertainties arising from the colour transformations, as the SSP model tracks were readily available for the CFHT/Megacam system. Fig. 4 shows that all clusters with the exception of Hodge IV in NGC 147 are metal poor with [Fe/H] $\lesssim -1.25$ dex. If Hodge IV is as metal-rich as we infer, it would be rather interesting. However we note that it is the second faintest cluster in NGC 147 and appears irregular in shape in the MegaCam imaging (see Fig. 2), while close to the detection limit in the near-IR data. Although one of the first clusters to be discovered in NGC 147 (Hodge 1976), high-resolution images of this object do not yet exist. Even with high-quality ground-based data such as PAndAS, it is difficult to confirm it is a genuine GC and not, for example, an asterism in the NGC 147 field.

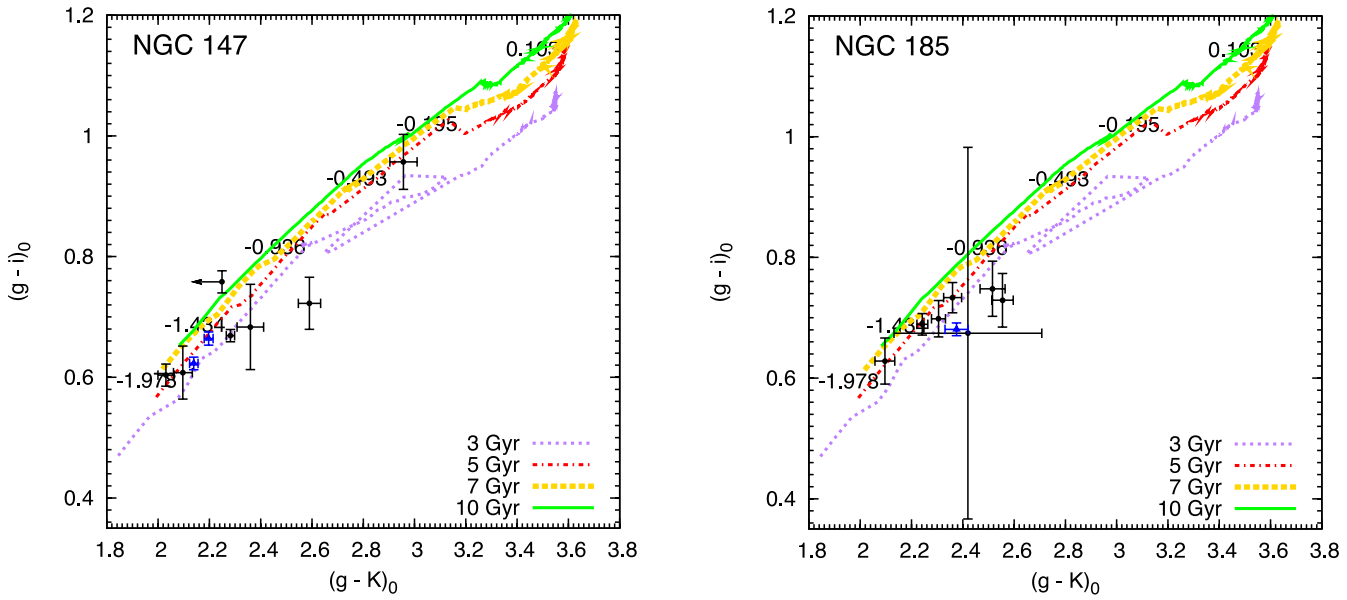

Figure 4. $(g - i)_0$ versus $(g - K)_0$ colours of GCs in NGC 147 (left) and NGC 185 (right) overlaid on top of isochrones from Marigo et al. (2008). The corresponding metallicity ([Fe/H]) values are indicated. The newly discovered GCs are marked as blue triangles. All but one cluster is found to be metal poor, while the age is more difficult to constrain.

Downloaded from http://mnras.oxfordjournals.org/ at The Australian National University on December 20, 2013

The ages of the clusters are more difficult to estimate. At face value, it appears that half of the GCs are old and half are of intermediate age. However, inspecting the clusters that lie on the young to intermediate-age tracks, it is found that they are often located in or near the main bodies of their host galaxies. As discussed earlier, these regions are very crowded and often have strong non-linear background gradients that can skew the colours of the GCs. This is certainly an issue for Hodge I in NGC 147 which has a redder $(g - K)_0$ colour than any of the tracks shown. The method of photometric age estimation is not particularly accurate even when free of these complications so we hesitate to claim we have found evidence for the presence of intermediate-age GCs. Furthermore, due to the way the SSP model isochrones are calibrated, small changes in either of the colours used in Fig. 4 will drastically affect their age estimates, while only minimally impacting their metallicity estimates.

Another outlier in Fig. 4 is GC-SD10 in NGC 147 which has a redder $(g - i)_0$ and bluer $(g - K)_0$ colour than any of the tracks. This object is the faintest out of all the clusters known in the two dEs and was not detected in our *K*-band imaging. The quoted *K*-band magnitude represents an upper limit, suggesting that the actual $(g - K)_0$ colour must lie bluewards of the point in Fig. 4. Although these colours seem unusual, GC-SD10 has been spectroscopically confirmed by Sharina & Davoust (2009) as a GC in NGC 147. Finally, even though the measured colours put FJJ III on the model tracks in Fig. 4, the accompanying uncertainties make constraining the age and metallicity of this cluster nearly impossible.

An alternative way to determine the metallicities of GCs is to use empirical colour–metallicity relations. We adopt the relationship derived by Kissler-Patig, Brodie & Minniti (2002) (equation 1), calibrated using 129 M31 globulars that have $E(B - V) < 0.27$, to further constrain the metal content of the NGC 147 and NGC 185 GC systems. This relationship is valid over the interval $-2.3 <$ [Fe/H] < -0.2 dex.

$$[\mathrm{Fe/H}] = (V - K) \times 1.82 \pm 0.11 - 5.52 \pm 0.26. \quad (1)$$

Table 6 shows the metallicities derived with the above relation and affirms our conclusion that the clusters are all indeed metal poor. Although we do not use our spectra to derive metallicities here, we note that the similarly strong Balmer lines visible in Fig. 1 for PA-N147-1 and PA-N147-2 support the similar metallicities derived from their broad-band colours. There is also a hint at a radial metallicity trend with GCs with projected radii >0.55 kpc having systematically lower [Fe/H] values by ∼0.6 dex compared to the central population. For comparison, Table 6 also shows metallicities for some of the previously known GCs derived from spectroscopic studies (Da Costa & Mould 1988; Sharina et al. 2006; Sharina & Davoust 2009), and from colour–magnitude diagram isochrone fitting (Sharina et al. 2006). There is generally a good agreement with past studies, lending further confidence to our metallicity estimates. The only exception is FJJ VII in NGC 185 for which a difference larger than 1 dex is seen between our measurements and the spectroscopic measurements of Sharina et al. (2006). We currently have no explanation for this.

Table 6. [Fe/H] values for GCs in NGC 147 and NGC 185. Columns refer to: (a) values obtained using the colour–metallicity relation from Kissler-Patig et al. (2002); (b) Da Costa & Mould (1988); (c) Sharina et al. (2006); Sharina & Davoust (2009); (d) Sharina et al. (2006). Superscripts refer to: (1) spectroscopic study; (2) isochrone fitting. Sharina et al. (2006) originally presented [Z/H] values which were converted to [Fe/H] via the relation from Salaris & Cassisi (2006).

ID	[Fe/H](a) (dex)	[Fe/H](b)[1] (dex)	[Fe/H](c)[1] (dex)	[Fe/H](d)[2] (dex)
Hodge I	-1.3 ± 0.4	-1.9 ± 0.15	-1.0 ± 0.5	...
Hodge II	-1.7 ± 0.4	-2.5 ± 0.25	-1.6 ± 0.5	...
Hodge III	-2.1 ± 0.3	...	-1.8 ± 0.5	-2.0 ± 0.1
Hodge IV	-0.7 ± 0.4	...	...	...
GC-SD5	-2.2 ± 0.3	...	-1.7 ± 0.3	...
GC-SD7	-1.8 ± 0.3	...	-1.6 ± 0.2	...
GC-SD10	-1.9 ± 0.4	...	...	...
PA-N147-1	-2.0 ± 0.3	...	...	...
PA-N147-2	-1.9 ± 0.3	...	...	...
PA-N147-3	...	...	...	...
FJJ I	-1.3 ± 0.4	-1.4 ± 0.10	-1.2 ± 0.4	-1.6 ± 0.2
FJJ II	-1.4 ± 0.4	-1.2 ± 0.25	...	-2.1 ± 0.2
FJJ III	-1.5 ± 0.5	-1.7 ± 0.15	-1.4 ± 0.6	-2.0 ± 0.1
FJJ IV	-2.1 ± 0.3	-2.5 ± 0.25	-1.6 ± 0.5	-2.0 ± 0.2
FJJ V	-1.8 ± 0.3	-1.8 ± 0.15	-1.1 ± 0.6	-1.5 ± 0.1
FJJ VII	-1.7 ± 0.4	...	-0.4 ± 0.6	...
FJJ VIII	-1.9 ± 0.3	...	-1.1 ± 0.9	...
PA-N185	-1.6 ± 0.4	...	...	...

6.2 Comparison to other dwarf elliptical galaxies

An oft-used statistic when comparing GC systems hosted by different galaxies is the GC-specific frequency, $S_N = N_{\mathrm{GC}} \times 10^{0.4(M_V+15)}$, where N_{GC} is the total number of GCs in the system, and M_V is the integrated absolute *V* magnitude of the host galaxy (Harris & van den Bergh 1981). This quantity can be thought of as the formation efficiency of GCs relative to field stars, although the interpretation is more complicated if one considers that fractions of these populations may have been accreted rather than formed in situ. In the case of dwarf galaxies, the GC specific frequency is poorly constrained at present due to incompleteness in terms of imaging and GC detection, but it is critical for understanding what kinds of dwarf galaxies may contribute GCs to the haloes of more massive systems. Significant effort has been made to constrain this value for dEs and past surveys have focused mainly on dwarf galaxies that reside in dense environments, such as the Fornax and Virgo clusters (Durrell et al. 1996; Miller et al. 1998; Lotz, Miller & Ferguson 2004; Miller & Lotz 2007; Peng et al. 2008). The study by Miller & Lotz (2007) found an overall trend of increasing S_N with increasing M_V (decreasing galaxy luminosity), which has also been found in dwarf irregulars although with smaller samples (Seth et al. 2004; Georgiev et al. 2008, 2010). Peng et al. (2008) find dwarf galaxies with the highest S_N values in their sample to be within 1 Mpc of the Virgo cluster core, which they interpret as an environmental effect. However, these authors also find that dEs within 40 kpc of the most massive galaxies in the Virgo cluster have few or no GCs, suggesting that they have probably been stripped away by the tidal forces from the central hosts.

Using our updated GC census, the specific frequencies for NGC 147 and NGC 185 were recalculated and found to be 8 ± 2 and 5.5 ± 0.5, respectively. This is a slight increase from the previous values which were 6 ± 2 for NGC 147 and 4.8 ± 0.5 for NGC 185. The uncertainties quoted for NGC 147 allow for the possibility of Hodge IV and SD-10 not being genuine GCs, as well as the uncertainty in the galaxy luminosity. In the case of NGC 185, only the uncertainty in the galaxy luminosity was taken into account. Fig. 5 shows the S_N versus M_V values for dEs observed in the Fornax and Virgo clusters and in the Leo group, taken from the studies of Miller & Lotz (2007) and Peng et al. (2008). The error bars are due to the

Downloaded from http://mnras.oxfordjournals.org/ at The Australian National University on December 20, 2013

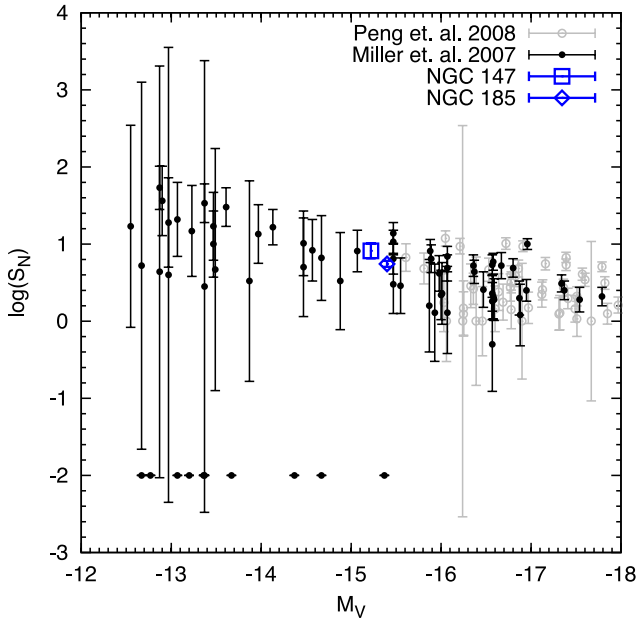

Figure 5. Plot of $\log(S_N)$ versus M_V for dEs in the Fornax and Virgo clusters, and in the Leo group, taken from the studies by Miller & Lotz (2007)(filled points) and Peng et al. (2008)(open grey points). Galaxies which do not host GCs are given $\log(S_N) = -2$ in order to distinguish them on the plot. Overplotted are the corresponding S_N values of NGC 147 and NGC 185.

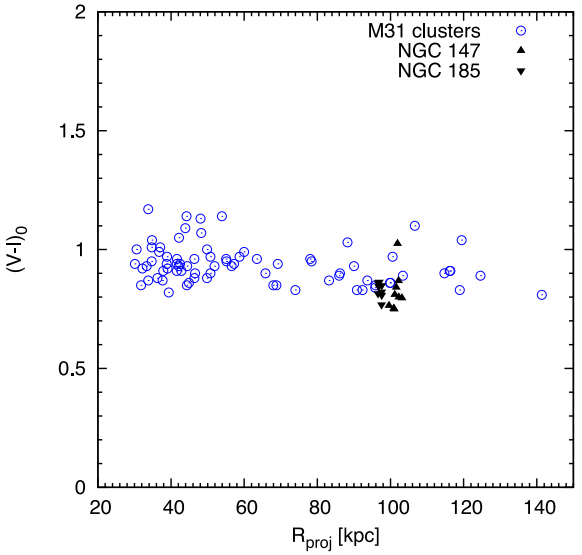

Figure 6. Plot of $(V - I)_0$ versus $R_{\rm proj}$ showing the M31 GCs that have projected radii larger than 30 kpc, together with the NGC 147 and NGC 185 GCs. Data were taken from the Revised Bologna Catalogue (Galleti et al. 2004) and Huxor et al. (in preparation). The colour similarity supports the suggestion that the M31 outer halo GCs could have been accreted from objects like NGC 147 and NGC 185.

uncertainty in the host galaxy luminosity and the uncertainty in the total number of GCs found around each galaxy, which has been corrected for background contaminants and spatial incompleteness. In the same figure overplotted are the updated S_N values for NGC 147 and NGC 185. The S_N values are within the range found for dEs of comparable luminosity observed by Miller & Lotz (2007), albeit residing in different environments, and appear to follow the trend of increasing S_N value with decreasing galaxy luminosity.

Another interesting property shared by the GC systems of NGC 147 and NGC 185, and the GC systems of dE galaxies found in rich environments, is their optical colours. The mean $(V - I)_0$ colours of NGC 147 and NGC 185 GCs are 0.85 and 0.84 with standard deviations of 0.09 and 0.03, respectively. In their study of dEs in the Fornax and Virgo galaxy clusters, Lotz et al. (2004) have reported the peak of the mean $(V - I)_0$ colour distribution to be 0.90 for galaxies with absolute magnitudes between −15.0 and −16.0, and 0.85 for galaxies with absolute magnitude between −14.0 and −15.0. This makes the GC systems of NGC 147 and NGC 185 nearly indistinguishable from those hosted by similar luminosity dEs in rich clusters, suggesting that the large-scale present-day environment has little impact on either S_N or mean optical colour.

6.3 Comparison to M31 halo globular clusters

Detailed surveys (e.g. Ferguson et al. 2002; McConnachie et al. 2009; Richardson et al. 2011) have revealed complex substructure in the halo of M31, consisting of loops, streams and filaments. This inhomogeneous halo is thought to have formed over an extended period of time via the accretion and disruption of dwarf galaxies. M31 also hosts an extended population of GCs, with clusters found up to distances of 200 kpc from its centre (Mackey et al. 2010a; Huxor et al. 2011). Evidence that the outer halo GC system may have formed predominantly by accretion was hinted at by the radial number density profile (see fig. 7 in Huxor et al. 2011). The profile has the form of a broken power law, with characteristic flattening occurring beyond a projected radius of ∼30 kpc. Such a behaviour is found in the stellar haloes of simulated galaxies that form via a combination of accretion and in situ star formation (Abadi, Navarro & Steinmetz 2006), with the break in the power law marking the point beyond which the bulk of the matter has been accreted.

More compelling evidence for an accretion origin comes from the fact that GCs in the outer halo are spatially correlated with the extended substructure of M31 (Mackey et al. 2010b). Statistical tests have shown that GCs preferentially project on top of stellar streams, with the probability of this being due to chance alignment being less than 1 per cent. On this basis, it is argued that over 80 per cent of the GCs found beyond 30 kpc from the centre of M31 have probably been donated by captured and disrupted dwarf galaxies. The fact that there is a significant number of dwarf galaxies in the halo of M31 (Richardson et al. 2011), where a few of the more luminous satellites are known to host GCs, shows that the halo is still actively evolving.

If the majority of the M31 halo GCs were indeed donated by captured dwarf galaxies, it might be expected that they share the some properties with the GCs hosted by NGC 147 and NGC 185. Fig. 6 displays the $(V - I)_0$ colours as a function of $R_{\rm proj}$ from the centre of M31 for the GCs hosted by NGC 147 and NGC 185. We also show confirmed M31 GCs that have $R_{\rm proj} > 30$ kpc taken from the Revised Bologna Catalogue (Galleti et al. 2004) and Huxor et al. (in preparation). The M31 GCs have been de-reddened using extinction coefficients from Schlegel et al. (1998). One can see that the GCs found around the two dwarf galaxies fit comfortably in the range of $(V - I)_0$ colours measured for their M31 halo counterparts. Although this does not prove that the M31 halo GCs have been accreted by systems like NGC 147 and NGC 185, it demonstrates that this idea is not inconsistent with the data. In terms of the number of GCs they currently host, only about eight NGC 147 or 185 systems would be needed to create almost the entire M31 halo

Downloaded from http://mnras.oxfordjournals.org/ at The Australian National University on December 20, 2013

GC population that consists of ∼80 clusters. Such accretions would also donate $\sim 5.4 \times 10^8$ $L_\odot$ of stellar light, consistent with estimates of the halo luminosity (Irwin et al. 2005).

7 SUMMARY

We have presented the results of a new search for remote GCs around the M31 satellites, NGC 147 and NGC 185, using data from PAndAS. The search resulted in the discovery of four new GCs, three of which are located close to NGC 147, while one is near NGC 185. Probability arguments and newly obtained radial velocities indicate that these objects are likely to belong to the dwarfs and not the M31 halo. Our findings serve as another example of the importance of studying galaxies beyond their optical boundaries.

We present the first homogeneous optical and near-IR photometry for the entire GC systems of these two dwarf galaxies. We use this to constrain the GC ages and metallicities via the use of colour–colour plots and empirical colour–metallicity relations, finding that, in general, the clusters are old and metal poor ([Fe/H] $\lesssim -1.25$ dex).

The mean colours of the GCs hosted by NGC 147 and NGC 185 are found to lie at the peak of the colour distribution of the GC systems belonging to dEs in the Fornax and Virgo galaxy clusters, despite a large difference in the environments in which they reside. Their S_N values are consistent with the trend of increasing GC-specific frequency with decreasing galaxy luminosity generally observed for dwarf galaxies, regardless of their type, and in a variety of environments. The close similarity between the $(V - I)_0$ colours of the GCs belonging to these two dwarf galaxies and those belonging to the M31 outer halo is consistent with the idea that accretion of the former could have contributed to the assembly of the latter.

ACKNOWLEDGEMENTS

The work of APH was partially supported by Sonderforschungsbereich SFB 881 'The Milky Way System' of the German Research Foundation (DFG). ADM is grateful for support from the Australian Research Council through an Australian Research Fellowship (Discovery Projects grant: DP1093431). We thank the CFHT staff for their support and helpfulness throughout the PAndAs project. Based on observations obtained with MegaPrime/MegaCam, a joint project of CFHT and CEA/DAPNIA, at the CFHT which is operated by the National Research Council (NRC) of Canada, the Institut National des Science de l'Univers of the Centre National de la Recherche Scientifique (CNRS) of France, and the University of Hawaii. This work is based in part on data products produced at TERAPIX and the Canadian Astronomy Data Centre as part of the CFHT Legacy Survey, a collaborative project of NRC and CNRS. Based on observations made with the 4.2-m William Herschel Telescope operated on the island of La Palma by the Isaac Newton Group in the Spanish Observatorio de Roque de los Muchachos of the Instituto de Astrofisica de Canarias. The United Kingdom Infrared Telescope is operated by the Joint Astronomy Centre on behalf of the Science and Technology Facilities Council of the UK.

REFERENCES

Abadi M. G., Navarro J. F., Steinmetz M., 2006, MNRAS, 365, 747
Baade W., 1944, ApJ, 100, 147
Battinelli P., Demers S., 2004, A&A, 417, 479
Bellazzini M., Ferraro F. R., Ibata R., 2003, AJ, 125, 188
Bender R., Paquet A., Nieto J.-L., 1991, A&A, 246, 349
Bertin E., 2009, Memorie della Societa Astronomica Italiana, 80, 422
Boulade O. et al., 2003, in Iye M., Moorwood A. F. M., eds, Proc. SPIE Vol. 4841, Instrument Design and Performance for Optical/Infrared Ground-based Telescopes. SPIE, Bellingham, p. 72
Brodie J. P., Strader J., 2006, ARA& A, 44, 193
Bruzual G., Charlot S., 2003, MNRAS, 344, 1000
Butler D. J., Martínez-Delgado D., 2005, AJ, 129, 2217
Casali M. et al., 2007, A&A, 467, 777
Chies-Santos A. L., Larsen S. S., Kuntschner H., Anders P., Wehner E. M., Strader J., Brodie J. P., Santos J. F. C., 2011, A&A, 525, A20
Cioni M.-R. L. et al., 2008, A&A, 487, 131
Collins M. L. M. et al., 2013, ApJ, 768, 172
Conn A. R. et al., 2012, ApJ, 758, 11
Corwin H. G., Jr, Buta R. J., de Vaucouleurs G., 1994, AJ, 108, 2128
Courteau S., van den Bergh S., 1999, AJ, 118, 337
Da Costa G. S., Mould J. R., 1988, ApJ, 334, 159
Davidge T. J., 2005, AJ, 130, 2087
Deveikis V., Narbutis D., Stonkutė R., Bridžius A., Vansevičius V., 2008, Balt. Astron., 17, 351
Dotter A., Sarajedini A., Anderson J., 2011, ApJ, 738, 74
Durrell P. R., Harris W. E., Geisler D., Pudritz R. E., 1996, AJ, 112, 972
Ferguson A. M. N., Irwin M. J., Ibata R. A., Lewis G. F., Tanvir N. R., 2002, AJ, 124, 1452
Ford H. C., Jacoby G., Jenner D. C., 1977, ApJ, 213, 18
Galleti S., Federici L., Bellazzini M., Fusi Pecci F., Macrina S., 2004, A&A, 416, 917
Geha M., van der Marel R. P., Guhathakurta P., Gilbert K. M., Kalirai J., Kirby E. N., 2010, ApJ, 711, 361
Geisler D., Armandroff T., da Costa G., Lee M. G., Sarajedini A., 1999, in Whitelock P., Cannon R., eds, IAU Symp. Vol. 192, The Stellar Content of Local Group Galaxies. Astron. Soc. Pac., San Francisco, p. 231
Georgiev I. Y., Goudfrooij P., Puzia T. H., Hilker M., 2008, AJ, 135, 1858
Georgiev I. Y., Puzia T. H., Goudfrooij P., Hilker M., 2010, MNRAS, 406, 1967
Gilbert K. M. et al., 2012, ApJ, 760, 76
Girardi L. et al., 2010, ApJ, 724, 1030
Harris W. E., 1996, AJ, 112, 1487
Harris W. E., van den Bergh S., 1981, AJ, 86, 1627
Hempel M., Geisler D., Hoard D. W., Harris W. E., 2005, A&A, 439, 59
Hodge P. W., 1974, PASP, 86, 289
Hodge P. W., 1976, AJ, 81, 25
Hodgkin S. T., Irwin M. J., Hewett P. C., Warren S. J., 2009, MNRAS, 394, 675
Huxor A. P., Tanvir N. R., Ferguson A. M. N., Irwin M. J., Ibata R., Bridges T., Lewis G. F., 2008, MNRAS, 385, 1989
Huxor A. P. et al., 2011, MNRAS, 414, 770
Huxor A. P., Ferguson A. M. N., Veljanoski J., Mackey A. D., Tanvir N. R., 2012, MNRAS, 429, 1039
Hwang N., Lee M. G., Lee J. C., Park W.-K., Park H. S., Kim S. C., Park J.-H., 2011, ApJ, 738, 58
Ibata R., Martin N. F., Irwin M., Chapman S., Ferguson A. M. N., Lewis G. F., McConnachie A. W., 2007, ApJ, 671, 1591
Irwin M. J. et al., 2004, in Quinn P. J., Bridger A., eds, Proc. SPIE Vol. 5493, Optimizing Scientific Return for Astronomy through Information Technologies. SPIE, Bellingham, p. 411
Irwin M. J., Ferguson A. M. N., Ibata R. A., Lewis G. F., Tanvir N. R., 2005, ApJ, 628, L105
Jang I. S., Lim S., Park H. S., Lee M. G., 2012, ApJ, 751, L19
King I., 1962, AJ, 67, 471
Kissler-Patig M., Brodie J. P., Minniti D., 2002, A&A, 391, 441
Koposov S. et al., 2007, ApJ, 669, 337
Kriek M. et al., 2010, ApJ, 722, L64
Law D. R., Majewski S. R., 2010, ApJ, 718, 1128
Lee M. G., Freedman W. L., Madore B. F., 1993, AJ, 106, 964
Lewis G. F. et al., 2013, ApJ, 763, 4
Lotz J. M., Miller B. W., Ferguson H. C., 2004, ApJ, 613, 262
McConnachie A. W., 2012, AJ, 144, 4

Downloaded from http://mnras.oxfordjournals.org/ at The Australian National University on December 20, 2013

McConnachie A. W., Irwin M. J., Ferguson A. M. N., Ibata R. A., Lewis G. F., Tanvir N., 2005, MNRAS, 356, 979
McConnachie A. W. et al., 2009, Nat, 461, 66
McConnachie A. W., Ferguson A. M. N., Irwin M. J., Dubinski J., Widrow L. M., Dotter A., Ibata R., Lewis G. F., 2010, ApJ, 723, 1038
Mackey A. D. et al., 2006, ApJ, 653, L105
Mackey A. D. et al., 2010a, MNRAS, 401, 533
Mackey A. D. et al., 2010b, ApJ, 717, L11
Maraston C., 1998, MNRAS, 300, 872
Marigo P., Girardi L., Bressan A., Groenewegen M. A. T., Silva L., Granato G. L., 2008, A&A, 482, 883
Martínez-Delgado D., Aparicio A., Gallart C., 1999, AJ, 118, 2229
Miller B. W., Lotz J. M., 2007, ApJ, 670, 1074
Miller B. W., Lotz J. M., Ferguson H. C., Stiavelli M., Whitmore B. C., 1998, ApJ, 508, L133
Peng E. W. et al., 2008, ApJ, 681, 197
Puzia T. H., Zepf S. E., Kissler-Patig M., Hilker M., Minniti D., Goudfrooij P., 2002, A&A, 391, 453
Regnault N. et al., 2009, A&A, 506, 999
Richardson J. C. et al., 2011, ApJ, 732, 76
Salaris M., Cassisi S., 2006, The Observatory, 126, 306
Saviane I., Rosenberg A., Piotto G., Aparicio A., 2000, A&A, 355, 966
Schlegel D. J., Finkbeiner D. P., Davis M., 1998, ApJ, 500, 525
Seth A., Olsen K., Miller B., Lotz J., Telford R., 2004, AJ, 127, 798
Sharina M., Davoust E., 2009, A&A, 497, 65
Sharina M., Afanasiev V., Puzia T., 2006, MNRAS, 372, 1259
van den Bergh S., 1998, AJ, 116, 1688
Vazdekis A., Sánchez-Blázquez P., Falcón-Barroso J., Cenarro A. J., Beasley M. A., Cardiel N., Gorgas J., Peletier R. F., 2010, MNRAS, 404, 1639
Veljanoski J. et al., 2013, ApJ, 768, L33
Watkins L. L., Evans N. W., van de Ven G., 2013, MNRAS, 430, 971
West M. J., Côté P., Marzke R. O., Jordán A., 2004, Nat, 427, 31
Yi S., Demarque P., Kim Y.-C., Lee Y.-W., Ree C. H., Lejeune T., Barnes S., 2001, ApJS, 136, 417
Young L. M., 2001, AJ, 122, 1747
Young L. M., Lo K. Y., 1997, ApJ, 476, 127

APPENDIX A: REVIEW OF THE LITERATURE ON THE NGC 147 AND NGC 185 GC SYSTEMS

The following is a short review of the discovery history and the nomenclature of the GCs hosted by NGC 147 and NGC 185. The motivation for this is to highlight some inconsistencies in the literature that we discovered while this paper was in preparation. By doing so, we hope to minimize the possibility of future confusion when studying the GCs of these two dEs.

The existence of GCs in both NGC 147 and NGC 185 was first reported by Baade (1944), who discovered two globulars in each of the galaxies. In his paper, the clusters were not named and coordinates were provided only for the ones hosted by NGC 185 and in terms of relative positions (measured on photographic plates) from the galaxy centre.

Hodge (1974) reported the discovery and presented photometry of five GCs in NGC 185, two of which were those previously discovered by Baade (1944). These clusters were simply labelled 1–5. While their coordinates were not provided, a finding chart was shown.

Two years later, Hodge (1976) published a paper on the structure of NGC 147, in which the discovery and photometry of two additional GCs bound to this galaxy were presented, alongside the two clusters previously discovered by Baade (1944). Once again, no coordinates for any of these objects were given, but a finding chart was published, on which the clusters are labelled 1–4. In the literature, these clusters are now known as Hodge I–IV.

In an appendix to their paper on planetary nebulae in NGC 147 and NGC 185, Ford et al. (1977) revisited the GC systems of the two dEs. In addition to the GCs already discovered by Baade and Hodge around NGC 185, they presented the discovery of an additional four clusters from their photographic plates, while also discarding the object labelled by Hodge (1974) as '2' as a GC. In Ford et al. (1977), the objects are numbered I–VIII but the counting does not follow the pattern started by Hodge (1974). This nomenclature has propagated through the literature, and these clusters are referred to as FJJ I–VIII in recent publications. In addition, equatorial coordinates together with a finding chart were also published for the entire sample of GCs described by Ford et al. (1977).

Ford et al. (1977) also revisited the GC system of NGC 147. They recovered the objects already identified by Hodge (1976) as globulars and did not find any new members belonging to this system. They showed a finding chart and a table with equatorial coordinates for the three brightest globulars in this galaxy. Their finding chart is identical to the one published by Hodge (1976) in terms of the labelling and positions of the GCs: Hodge II is south of Hodge I and Hodge III is south of Hodge II. However, in their table 9 that lists the clusters' coordinates, the positions of Hodge II and Hodge III are swapped: Hodge II is listed to be south of Hodge III. This unintentional oversight is most probably the main reason for many inconsistencies in the more recent literature.

A paper published by Da Costa & Mould (1988) presented spectroscopic data and metal abundances of the GCs hosted by NGC 147 and NGC 185. Regarding the NGC 185 system, they presented *V*-band photometry taken from Hodge (1974) and spectroscopic data for clusters FJJ I–V, as well as Hodge 2 that Ford et al. (1977) classified not to be a cluster. For cluster FJJ IV which was not listed amongst the GC candidates by Hodge (1974) the *V* magnitude was estimated by eye. Analysing the cluster spectra, Da Costa & Mould (1988) showed that Hodge 2 is indeed a galaxy at redshift $z = 0.04$ and not a GC.

Regarding the NGC 147 system, Da Costa & Mould (1988) took spectra only of Hodge I and Hodge III. In their table 1 they listed the photometric *V* magnitude of these two clusters as reported by Hodge (1976). They did not list coordinates for any of the clusters but stated that the centres of the clusters were taken from Ford et al. (1977). This probably means that they presented metal abundances of Hodge II rather than Hodge III. There was no indication that Da Costa & Mould (1988) noticed the oversight made by Ford et al. (1977), and in Table 6 in our paper it is assumed that they have not.

Geisler et al. (1999) observed all but one cluster in NGC 185 with the *Hubble Space Telescope* (*HST*), that were known at that time. The cluster which was not observed was FJJ VIII. They found that FJJ VI is not a GC but an elliptical galaxy. All other cluster candidates that were observed were confirmed to be genuine GCs.

In more recent literature, Sharina et al. (2006) revisited the GC systems of NGC 147 and NGC 185 using *HST*/WFPC2 imagery and spectroscopy taken with the SCORPIO spectrograph. They did not provide coordinates for any of the clusters, but they did provide finding charts. In the case of NGC 147, they had the positions of Hodge II and Hodge III reversed compared to the original publication by Hodge (1976), so it is highly likely the data and results presented for Hodge II actually refer to Hodge III and vice versa. In their table 2, they have taken the *V* magnitudes of what they label as Hodge I and Hodge III from the original paper by Hodge (1976), while the *V* magnitude of their Hodge II is taken from Hodge (1974) even though this paper analysed only clusters hosted by NGC 185

Downloaded from http://mnras.oxfordjournals.org/ at The Australian National University on December 20, 2013

and did not list photometric values for any cluster in NGC 147. This made the cluster they label as Hodge II brighter than Hodge III, which is easily seen not to be the case with simple visual inspection of their *HST* images.

The most recent publication regarding the NGC 147 GC system is by Sharina & Davoust (2009). In their paper they announced the discovery of three new GCs. They presented a coordinate table and a finding chart, both having correct positions compared to the original. In addition, they also state that the identifiers of Hodge II and Hodge III were inverted by mistake in Sharina et al. (2006), meaning any values cited from the earlier publication are not assigned to the wrong object in Sharina & Davoust (2009).

Finally, in our paper we report the discovery of another three GCs hosted by NGC 147, and one hosted by NGC 185. Interestingly, all three of the new GCs in NGC 147 lie beyond areas previously imaged for GC searches, while the new GC in NGC 185 lies within the photographic plate region searched by Ford et al. (1977). We speculate that the outlying nature of this object coupled with its low luminosity caused it to be missed in the original study. The tables we present here reflect the original naming and correct coordinates for all previously known GCs, as well as these new discoveries.

This paper has been typeset from a TEX/LATEX file prepared by the author.

Downloaded from http://mnras.oxfordjournals.org/ at The Australian National University on December 20, 2013